Stochastic model for the motion of a particle on an inclined rough plane and the onset of viscous friction

G. G. Batrouni,[1,2] S. Dippel,[2] and L. Samson[1]
[1]*Groupe Matière Condensée et Matériaux, CNRS URA No. 804, Université de Rennes 1, 35042 Rennes Cedex, France*
[2]*Höchstleistungsrechenzentrum, Forschungszentrum, D-52425 Jülich, Germany*
(Received 12 December 1995)

Experiments on the motion of a particle on an inclined rough plane have yielded some surprising results. For example, it was found that the frictional force acting on the ball is viscous, i.e., proportional to the velocity rather than the expected square of the velocity. It was also found that, for a given inclination of the plane, the velocity of the ball scales as a power of its radius. We present here a one-dimensional stochastic model based on the microscopic equations of motion of the ball, which exhibits the same behavior as the experiments. This model yields a mechanism for the origins of the viscous friction force and the scaling of the velocity with the radius. It also reproduces other aspects of the phase diagram of the motion which we will discuss. [S1063-651X(96)08306-7]

PACS number(s): 46.10.+z, 46.30.Pa, 46.90.+s

I. INTRODUCTION

A mixture of particles with different sizes can segregate under a wide range of conditions and due to various mechanisms (usually a combination) such as the ''Brazil nut effect'' (the rise of large grains to the top due to shaking) [1], shear [2], percolation [3], convection [4], or surface flow [5]. Clearly the problems of mixing and segregation have important consequences for many industries. To understand this complicated phenomenon, it is easiest to study the effects of the various mechanisms separately, if possible.

In this paper we are interested in segregation due to flow which can be seen, for example, in sand piles. When grains with various sizes flow on the surface, one observes that the largest grains find their way to the bottom of the pile while the smaller ones are stopped farther uphill. This segregation is caused by the roughness of the underlying surface on which the grains are flowing. In a much simplified picture, one can consider the bulk of the sand pile as providing a rough substrate on which the surface grains are flowing and segregating. For experimental purposes, one can carry the simplification further and consider an inclined plane made rough by sticking beads of a given radius, r, for example glass or sifted sand, on contact paper and attaching it to the plane. This was done in a series of experiments [6–9] where various properties of the motion of balls down this plane were studied. We refer the reader to the references for details of the experiments and results. Here we will review some of the results before proceeding to our theoretical model.

Three regimes were found [8,9] for the motion of the ball down the plane: (A) A sticking or pinning regime where the ball comes to a sudden stop after traveling some distance, (B) a regime where the ball attains a steady state with a constant (on average) velocity independent of the initial release velocity, and (C) a jumping regime where the ball experiences big bounces and does not achieve a steady state on the 2-m-long plane used in the experiments. One expects that for a long enough plane, the ball will always reach a steady state, but even so, the nature of the motion in this regime appears to be different from that of region B. However, because of experimental difficulties, this regime remains mostly unstudied.

In region B, it was found that the constant (average) velocity satisfies $\langle v\rangle \propto R^{\alpha}\sin(\theta)$ [10]. This is a surprising result because it means that the force of friction acting on the ball is viscous, i.e., proportional to the velocity [6–9]. A straightforward argument suggests that the friction force should be quadratic in the velocity leading to a $\sqrt{\sin(\theta)}$ behavior: It is clear that the deceleration due to collisions is proportional to the number of collisions per second times the velocity loss per collision. The velocity loss per collision is proportional to the velocity itself, and one can argue that the average number of collisions per second is the velocity of the ball divided by the average distance between surface beads. This gives a friction force which is quadratic in the velocity, contrary to what is seen experimentally. Two assumptions that would lead to viscous friction are (1) the velocity loss per collision is a constant independent of the velocity, or (2) the number of collisions per second is a constant independent of the velocity. However, neither of these assumptions can be justified physically and the explanation should be sought elsewhere.

It is tempting to draw an analogy between the motion of a ball down a rough plane with peaks and troughs and the motion of particles in random potentials [11] using a Langevin equation to describe the dynamics. However, such an approach cannot explain the viscous dissipation because the viscous friction term is put in as an assumption from the start. In addition, even if one does assume the viscous force and pursues this approach, the scaling of the velocity with R, i.e., with the roughness which in this approach characterizes the random potential, is not correctly reproduced. The missing ingredient will be discussed in Sec. III. A different approach was taken in [7] where a Langevin equation, with the viscous dissipation and the velocity scaling with R built in, was used to study other aspects of the motion such as the stopping distance and its dependence on various parameters.

The approach we will take here is different still. We will

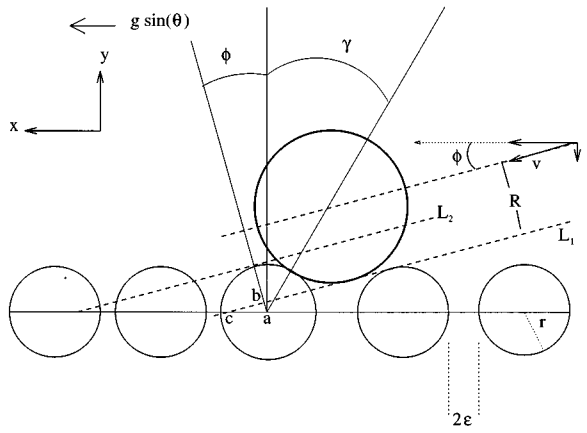

FIG. 1. Shows the geometry of the inclined line of disks, r, on which we release a disk R. The collision depicted is that for the largest negative value of γ, the contact angle.

consider the one-dimensional case, i.e., disks of radius r are randomly stuck on a line inclined at an angle θ with the horizontal, and on which is released a disk of radius R. We then consider the equations of motion of the disk, R, as it moves down the line, and make as many simplifying assumptions as is reasonable, eventually turning the deterministic equations into stochastic ones. Our goal in this is not to have a detailed microscopic agreement with experiments: That would be an unrealistic hope with a very simple model and is more the domain of detailed numerical simulations. Rather, our goal is to have a bare-bones stochastic model that agrees with experiments and reproduces various properties of the motion such as the viscous friction and the scaling of the velocity with R. With this model, we succeeded in finding a simple mechanism for the viscous force and the various scaling laws. In all this geometry plays a crucial role.

In Sec. II we will construct the model clearly stating all our assumptions, and in Sec. III we will compare our results with the experiments and make some comments. Section IV contains our conclusions.

II. THE MODEL

Figure 1 shows the geometry of the system. Disks of radius r are put in a straight line, the distance between the surfaces of two neighboring disks being 2ϵ, where ϵ is a random number between 0 and a maximum value, ϵ_M. This line is inclined an angle θ with respect to the horizontal, and we will take the direction parallel [perpendicular] to it as the x [y] direction. Therefore, the gravitational acceleration in the x [y] direction is $g\sin(\theta)$ [$-g\cos(\theta)$]. The big disk, radius R, moves from right to left with a velocity $\vec{v}$ and x and y components v_x and v_y, making an angle ϕ with the line of disks, $\sin(\phi)=|v_y|/|\vec{v}|$. As shown in Fig. 1, γ is the angle between the line perpendicular to the line of disks, and the line connecting the centers of the big and small disks at the point of contact. We will call this the angle of contact which, it should be emphasized, is different from the angle of incidence. Our sign convention is that when the collision is on that side of the small disk which faces the approaching big disk (as in the figure) $\gamma<0$, and when it is on the other side, $\gamma>0$.

Our first assumption is that we can ignore the rotation of the big disk as it moves down the line. Clearly this assumption is not justified if we are aiming at detailed microscopic comparison with experiments. For example, neglecting rotation means that v_t, the tangential velocity of the point of contact during a collision, is due entirely to the translational velocity of the disk. This is important quantitatively because μ_t, the tangential coefficient of restitution, depends on v_t (see below). However, molecular dynamics (MD) simulations have shown [12] that if we prevent the disk from rotating as it bounces down the line and have only dynamic friction acting as the tangential force, the qualitative features of the motion, such as the θ dependence of the velocity, do not change. Since we are interested here in the scaling properties of the motion, we will neglect the rotation. Therefore, with this assumption, the only effect of the size of the disk is to contribute geometrical constraints as we will see below.

Our second assumption is that after a collision, the velocity components normal and tangential to the small disk at the point of impact are related to the corresponding velocities before the collision by

$$|v_n'|=\mu_n|v_n|, \tag{1a}$$

$$v_t'=\mu_t v_t, \tag{1b}$$

where μ_n (μ_t) is the normal (tangential) coefficient of restitution. There are absolute value signs in Eq. (1a) but not Eq. (1b) because the coefficient of normal restitution is always positive while that for tangential restitution can be negative [see Eqs. (9a) and (9b)]. The angle of incidence, a_i (not shown in the figure), is of course given by $\cos(a_i)=|v_n|/|\vec{v}|$, and $\sin(a_i)=|v_t|/|\vec{v}|$, while the angle of reflection, a_r, is given by $\cos(a_r)=|v_n'|/|\vec{v}'|$, and $\sin(a_r)=|v_t'|/|\vec{v}'|$, where the primes denote values just after the collision. Now consider the big disk going down the inclined line colliding with the small disks, and let us examine the kth collision. Let the x and y velocities just before (after) the kth collision be $v_x(k)$ [$v_x'(k)$] and $v_y(k)$ [$v_y'(k)$]. It is easy to see from these definitions and the simple plane geometry that

$$v_n(k)=|v_y(k)|\cos(\gamma)-v_x(k)\sin(\gamma), \tag{2a}$$

$$v_t(k)=|v_y(k)|\sin(\gamma)+v_x(k)\cos(\gamma), \tag{2b}$$

keeping in mind our convention for the sign of γ. The x velocity after the kth collision is $v_x'(k)=|\vec{v}'|\sin(a_r+\gamma)$ which, after expanding the sine and using the above definitions of the angle of reflection, gives

$$v_x'(k)=\mu_t v_t\cos(\gamma)+\mu_n v_n\sin(\gamma). \tag{3}$$

Combining this with Eqs. (2a) and (2b) allows us to express the x velocity just after the kth collision in terms of the x and y velocities just before the collision as

$$v_x'(k)=v_x(k)(\mu_t\cos^2(\gamma)-\mu_n\sin^2(\gamma)) + |v_y(k)|(\mu_t+\mu_n)\sin(\gamma)\cos(\gamma). \tag{4a}$$

A similar argument for $v_y(k)$ gives

$$v_y'(k) = -v_x(k)(\mu_t+\mu_n)\sin(\gamma)\cos(\gamma) + |v_y(k)|(\mu_n\cos^2(\gamma)-\mu_t\sin^2(\gamma)). \quad (4b)$$

Our next assumption, which is supported by MD simulations [12,13], is that the motion of the disk is composed mainly of a series of small bounces with very little or no rolling which we will, therefore, ignore. This means that the kth collision will cause the disk to bounce and spend a time $\delta\tau(k)$ in the air during which it will experience x acceleration $g\sin(\theta)$. Therefore, its x velocity just before the $(k+1)$th collision is $v_x(k+1)=\delta\tau(k)g\sin(\theta)+v_x'(k)$, which, combined with Eq. (4a), gives

$$v_x(k+1) = \delta\tau(k)g\sin(\theta)+v_x(k)(\mu_t\cos^2(\gamma)-\mu_n\sin^2(\gamma)) + |v_y(k)|(\mu_t+\mu_n)\sin(\gamma)\cos(\gamma). \quad (5a)$$

What happens to the perpendicular velocity, v_y? If the disk, after the collision shown in Fig. 1, bounces up and lands on another small disk but at the same y value, its v_y just before the new collision is identical, in absolute value, to that just after the previous collision. In general, however, the y value will be different because the big disk will land on various different points of the small disks. However, since we are typically interested in $R/r \geqslant 3$, we see that the variations in y are very small. We can, therefore, make the simplifying assumption that $v_y(k+1)$, the y velocity just *before* collision $(k+1)$ equals $v_y'(k)$, the y velocity just *after* collision k [14]. We then have

$$v_y(k+1) = -v_x(k)(\mu_t+\mu_n)\sin(\gamma)\cos(\gamma) + |v_y(k)|(\mu_n\cos^2(\gamma)-\mu_t\sin^2(\gamma)). \quad (5b)$$

So, Eqs. (5a) and (5b) express the x and y velocities just before the $(k+1)$th collision in terms of those just before the kth collision. Although not written explicitly, to simplify the notation, it should not be forgotten that the contact angle γ appearing on the right-hand side of these equations is actually $\gamma(k)$, the angle for the kth collision. These equations are deterministic since, given the initial conditions, one can, in principle, calculate for all subsequent collisions the two terms that have not yet been specified, $\delta\tau(k)$ and $\gamma(k)$. Such a detailed microscopic approach is not our goal in this paper. Instead, we want to transform Eqs. (5a) and (5b) into stochastic processes by making γ a stochastic variable. To do that we need its distribution which must be based on the underlying microscopics of the collisions. To simplify the calculation of this distribution, we assume that the disk R collides with a given small disk only once. With this assumption, it is clear from Fig. 1 that for a given incident velocity $\vec{v}$ or, equivalently, for a given angle ϕ, the largest (positive) contact angle $\gamma_{max}(k)$ is obtained when the big disk collides with the small disk while tangent to the line L_2. For this case, $\gamma_{max}(k)=\phi(k)$. On the other hand, the smallest (i.e., the largest negative) $\gamma_{min}(k)$ is obtained for the case shown in the figure, with the big disk tangent to line L_1. This is a good approximation only for large values of R since then the moving disk does not go deep in the space between two surface disks. Since in the experiments, and therefore in this paper, $R \geqslant 2$, this approximation is reasonable. Notice that L_1 is tangent to the disk just to the right of the disk involved in the collision. This shows how disks cast velocity dependent ''shadows'' on their neighbors thus restricting the area available for a collision with a given bead. It is straightforward to show that

$$\sin(\gamma_{min}(k)) = \sin(\phi(k))\cos(\alpha(k)) - \cos(\phi(k))\sin(\alpha(k)), \quad (6a)$$

where

$$\cos(\alpha(k)) = 1-2\frac{r+\epsilon}{r+R}\sin(\phi(k)), \quad (6b)$$

and where $2(r+\epsilon)$ is the distance between the center of the disk under collision and that to its immediate right. Recall that ϵ is a uniformly distributed random number between 0 and some maximum value ϵ_M. This gives the range of the stochastic variable, $\gamma(k)$, to be between a maximum value, $\phi(k)$ [where $\sin(\phi(k))=v_y(k)/|\vec{v}(k)|$], and a minimum value given by Eqs. (6a) and (6b). But we still need its distribution. To this end, we assume that for a given collision, the point of disk R that is closest to line L_1 (in Fig. 1 it actually touches it) is equally likely to be anywhere between L_1 and L_2. The position of this point determines the value of the contact angle γ, and therefore knowing its probability distribution (which we assumed to be uniform) gives the probability distribution for γ. Using this, it is straightforward to show from the geometry that γ is given by

$$\sin(\gamma(k)) = \sin(\phi(k))\left(\frac{R+y\sin(\phi(k))}{r+R}\right) - \cos(\phi(k))\left[1-\left(\frac{R+y\sin(\phi(k))}{r+R}\right)^2\right]^{1/2}, \quad (7a)$$

where

$$y = \text{uniform random number} \in \left[\frac{r}{\sin(\theta)}-2(r+\epsilon), \frac{r}{\sin(\theta)}\right]. \quad (7b)$$

One sees that the distribution for γ is a function of the geometry (R, r, and ϵ) and the incoming velocities (v_x and v_y) which determine how much of the surface disk area is available for collision. The distribution given by Eqs. (7a) and (7b) is shown in Fig. 2.

Equations (5a), (5b), (7a), and (7b) define most of the stochastic model. We still need to specify $\delta\tau(k)$, the time between collisions, when energy is fed into the system. Perhaps a temptingly simple hypothesis is that $\delta\tau(k)=d/v_x'(k)$, where d is the average distance between the centers of the line disks. However, as explained in Sec. I, it is easy to see that this gives a friction force proportional to v_x^2, and not v_x. An alternative argument is to say that for a perfectly smooth surface, the time between bounces is given only by v_y [$\delta\tau(k)=2v_y'(k)/g\cos(\theta)$], and assume the same holds for the rough plane. Integrating the stochastic equa-

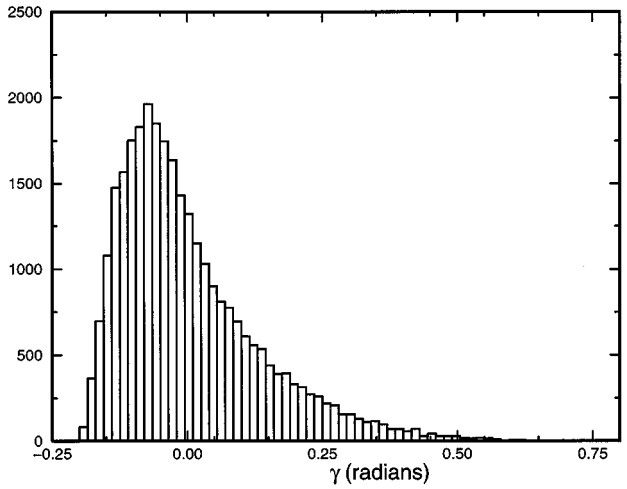

FIG. 2. A histogram showing the distribution of the stochastic variable γ (in radians) given by Eqs. (7a) and (7b). Recall that in our convention, $\gamma<0$ if the collision is as shown in Fig. 1, and $\gamma>0$ if it is on the other side of the perpendicular. $\sin(\theta)=0.3$, $R=0.3$ cm, $r=0.05$ cm, $\epsilon=0.01$ cm, $\mu_n=0.9$, $\mu=0.142$, and $\beta=0.45$. See Eqs. (5a), (5b), (7a), (7b), (8a), (8b), (9a), and (9b) for definitions of the parameters.

tions of motion with this assumption produces two types of solution depending on the parameters used: Either the ball energy is continuously dissipated until it comes to a complete stop, or the ball makes bigger and bigger jumps accelerating all the time and never reaching a stationary state. Clearly neither of these two possibilities for $\delta\tau(k)$ is realistic. Since the surface is rough, *both* v_x and v_y play a role in determining $\delta\tau(k)$. As we shall see below, the balance between v_x and v_y plays a crucial role in determining the properties of motion.

To motivate our choice for $\delta\tau(k)$ note, from Eqs. (4a) and (4b), that a collision with a negative γ transfers velocity from the x to the y direction, while the opposite happens for a positive γ. Furthermore, for a negative γ collision, the big disk has to jump *over* the small disk in order to continue its motion, while for a positive γ collision the big disk can *always* continue its motion. For these reasons, we assume that for a collision with γ negative (positive), $\delta\tau(k)$ is determined only by v_y (v_x). In other words, for $\gamma(k)<0$

$$\delta\tau(k)=\frac{2v_y'(k)}{g\cos(\theta)}, \tag{8a}$$

and for $\gamma(k)\geqslant 0$

$$\delta\tau(k)=\frac{2(r+\epsilon)}{v_x'(k)}. \tag{8b}$$

Note that in Eq. (8b) we are assuming that the distance traveled to the next collision is well approximated (on average) by $2(r+\epsilon)$. Of course in reality, v_x and v_y *together* determine the time between collisions. This can be calculated but would not reveal the underlying reasons for the viscous force which we are trying to explain. Equations (8a) and (8b) give a simplification that attempts to understand the separate roles of the parallel and perpendicular velocities.

The last ingredient in our model is the experimental observation that the tangential coefficient of restitution is strongly dependent on the angle of incidence [15], given by the normal (tangential) components of the velocity, v_n (v_t) [see Eqs. (2a) and (2b)]. It was found in Ref. [15] that the tangential coefficient of restitution is well parametrized by

$$\mu_t(k)=1-3.5(1+\mu_n)\mu\frac{v_n(k)}{v_t(k)}, \tag{9a}$$

in collisions that involve gross sliding, whereas in collisions that do not

$$\mu_t(k)=-\beta. \tag{9b}$$

In these equations, μ is the coefficient of friction, and β is the tangential coefficient of restitution in the absence of sliding. The normal and tangential velocities are given by Eqs. (2a) and (2b). We mention here that as a consequence of our ignoring the rotation of the big disk, the tangential velocity is given only in terms of the translational velocities v_x and v_y. However, rotation modifies the tangential (but not the normal) velocity and therefore the effective μ_t for each collision. This effective change in μ_t will lead to a different average velocity, but not to a qualitatively different behavior which is one justification for ignoring rotation. Note that ignoring rotation and its influence on the tangential velocity, v_t, means that the only way v_t can be changed by a collision is via dissipation. This dissipation is produced by a small amount of sliding and the concomitant friction, which is modeled mesoscopically by Eq. (9a). Therefore, in our model, it is Eq. (9a) that provides the tangential dissipation with no contribution from Eq. (9b).

Now, our stochastic process is completely defined by Eqs. (5a), (5b), (7a), (7b), (8a), (8b), (9a), and (9b). This stochastic process is nonlinear and cannot be solved exactly. However, the equations can be easily iterated numerically, and the statistical properties of the motion of the disk down the line studied in detail. The initial conditions are random choices for $v_x(1)$, $v_y(1)$, and $\gamma(1)$ from which everything else follows simply by generating the random number y. If a collision results in a negative value for v_x we consider the disk to have been pinned.

The equations defining our model can be further simplified by noting that all the angles are very small allowing us to expand all trigonometric functions to second order in γ. However, the resulting equations will still be nonlinear and require a numerical integration. The utility of such an expansion would be for approximate solutions, e.g., mean field.

III. RESULTS

In this section we compare the results of our model with the experiments. The first test of the model is whether it can reproduce the three experimentally found phases [6–9], the pinning phase A, the constant velocity phase B, where $\langle v_x\rangle \propto \sin(\theta)$, and the ''jumping'' phase C. Figure 3(a) shows $\langle v_x\rangle$ as a function of $\sin(\theta)$ for three values of R, the radius of the big disk. We clearly see regions that are linear in $\sin(\theta)$ through which we have fitted straight lines. Although

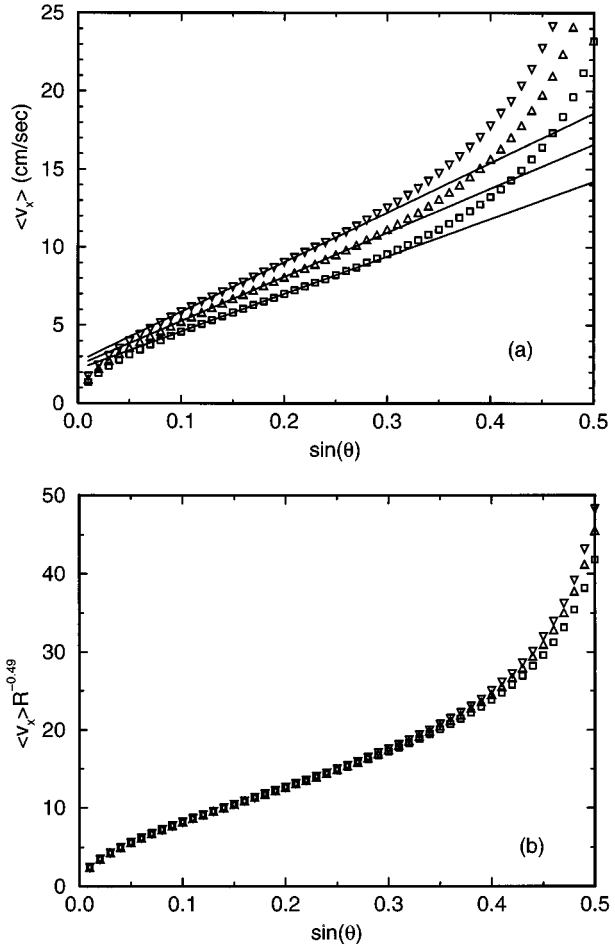

FIG. 3. (a) Shows the dependence of $\langle v_x \rangle$ (in cm/sec) on $\sin(\theta)$. There is a clear linear region in agreement with experiments. $R=3,4,5$ mm for $\square,\triangle,\triangledown$; $\mu=0.142$; $\mu_n=0.9$, $\beta=0.45$; $r=0.5$ mm. (b) Same as (a) but with the vertical axis scaled by $R^{-0.49}$.

we will not attempt to match our results exactly with experimental values, it is beneficial to see if the theoretical results are in reasonable general agreement with experiments. The linear regions stretch from about 4.5 to 14.5 degrees (the precise values depend on R, and for a given R they depend on the coefficients of friction and normal restitution), and the values of $\langle v_x \rangle$ are of the order of 5 to 15 cm/sec, all in very good general agreement with the experiments. Also in agreement with experiments, we found that the average velocity in region B does not depend on the initial velocity with which the ball was released. This is an important property of the motion in this region and does not apply in region C. When we scale the curves in Fig. 3(a) by a factor of $R^{-0.49}$ we get Fig. 3(b), which shows excellent scaling in the linear region, again in agreement with the experiments. The exponent we found, -0.49, differs from the experimental value [7,8], -1.4. Changing the parameters of the calculation, i.e., the values of the coefficients of restitution and friction, changes the exponents only a little and does not bring it close enough to the experimental value. We think that this difference could be due to the fact that the calculation is done in one dimension while the experiments are two dimensional. It might also be that our approximations, while maintaining the qualitative features of the physics, have changed this exponent.

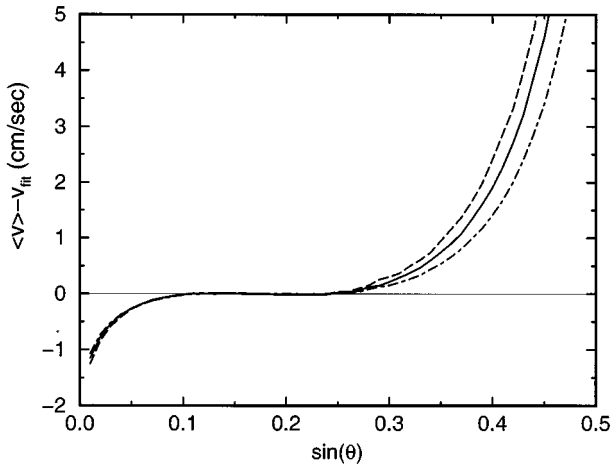

FIG. 4. Deviations of $\langle v_x \rangle$ from the straight line fits of Fig. 3(a). $R=3,4,5$ mm for the dot-dashed, solid, and dashed lines.

This insensitivity of the exponent to the values of the coefficients of restitution and friction explains the experimental result [16] that for a given value of θ, R, and r, the average velocity is practically independent of the material of the plane or the ball [17]. In other words, having fixed θ, R, and r, balls of plastic, glass, and steel, whose coefficients of restitution and friction are not very different, were found to have the same terminal velocity. Furthermore, this terminal velocity did not change when the surface of the plane was changed from glass beads, radius r, to sand with average grain radius r.

To check how linear these plots are, we show in Fig. 4 $\langle v_x \rangle - v_{fit}$, where v_{fit} is the value of the velocity given by the straight line fit to each of the curves. We see that for $\sin(\theta)$ between about 0.1 and 0.25 the deviation is extremely small and the linear fit is excellent. For $\sin(\theta)$ larger than about 0.25 we see that the $\langle v_x \rangle$ increases faster than linearly. We take this as the definition of region C, which for brevity we will call the ''jumping'' regime because, as mentioned in the Introduction, the motion is dominated by large jumps as compared with the small bounces in region B. We see from Fig. 4 that the largest disk, dashed line, enters the jumping regime earlier and faster than the smaller ones. This is in agreement with experimental phase diagrams [7,8] and with numerical simulations [18,12]. Experiments have also shown that as the ball approaches the jumping regime, C, it exhibits intermittent behavior where it still has a constant average velocity but it shows bursts of acceleration and deceleration. Figure 5 shows a plot of distance traveled as a function of time for $\sin(\theta)=0.53$ from our model. Bursts of acceleration and deceleration are clearly seen. This intermittency gets much more dramatic as one gets closer to the jumping regime (increasing θ) before the motion gets completely destabilized. The origin of a burst of acceleration is a particularly big bounce, due to high speed and a large negative γ, where the disk spends a long time in the air, gaining a lot of energy, which it has difficulty losing. Then comes another big shock that dissipates a lot of the energy, and the disk regains its former slower velocity. This mechanism can be inferred from the sharpness of slope changes (i.e., velocity changes) in Fig. 5.

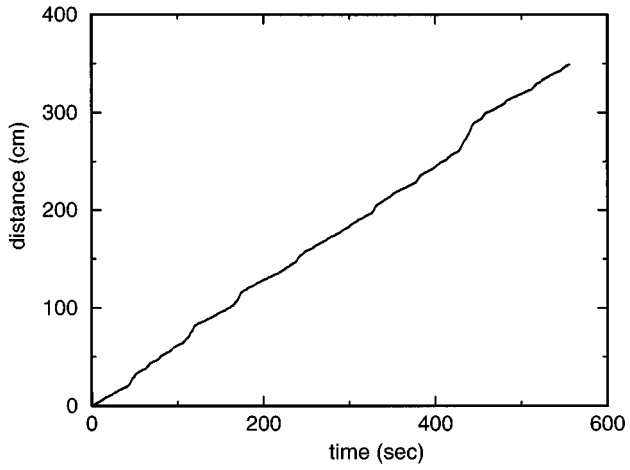

FIG. 5. Distance traveled (in meters) as a function of time (in seconds) for a disk of radius $R=4$ mm and an inclination angle $\sin(\theta)=0.53$. All the other parameters are as in Figs. 3(a) and 3(b). The slope gives the velocity parallel to the inclined line and exhibits bursts of acceleration and deceleration.

Figure 4 also shows that as θ is decreased, the average velocity decreases and eventually exhibits a sublinear dependence before it enters the pinning regime. To study the transition between the pinning regime A and the constant velocity regime B, we release several disks for each value of θ and R (keeping r fixed) one after the other and with slightly different initial velocities. We consider the system in the pinning regime when at least half the disks are stopped. As is clear from Fig. 6, the pinning regime quickly shrinks (i.e., moves towards smaller θ), and then disappears as R is increased. This agrees with the experiments, although in our calculation region A disappears faster.

Experiments have indicated [8,19] that $\langle v_x \rangle$ does not depend on the ratio R/r alone. For example, Jan *et al.* [19] showed that changing R while keeping the ratio R/r fixed (they kept $R=r$), $\langle v_x \rangle$ grows like $\sqrt{R}$. Figure 7 shows

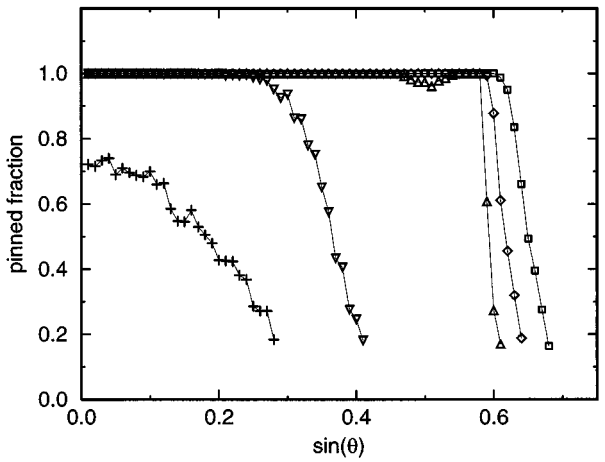

FIG. 6. Fraction of pinned disks as a function of the inclination angle. $R=2$, 2.2, 2.4, 2.6, 2.7 mm for $\square, \diamond, \triangle, \triangledown, +$. The other parameters are as in Figs. 3(a) and 3(b). For each data point 500 disks were released.

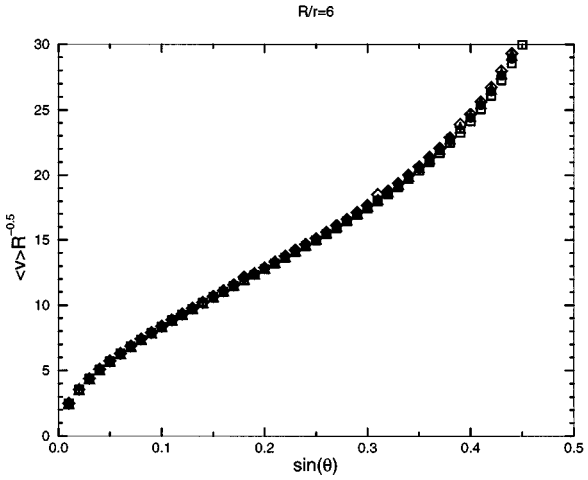

FIG. 7. Scaling of $\langle v_x \rangle$ with R when R/r is kept constant. The data collapse is for $R=3,4.5,6,7.5,9$ mm and the same parameters as in Figs. 3(a) and 3(b).

$\langle v_x \rangle R^{-0.5}$ as a function of $\sin(\theta)$ for $R=3,4.5,6,7.5,9$ mm and R/r fixed at 6. The figure exhibits excellent data collapse with an exponent that agrees with the experimental value. The same scaling is observed in MD simulations [12].

So, we see that the simplified stochastic model presented here has reproduced remarkably well all the features of the experimental results. But what is the mechanism behind the linear dependence on $\sin(\theta)$ and the scaling with R? As mentioned in Sec. II, if one argues that the time between collisions, $\delta\tau$, is set by the parallel velocity, v_x, one gets a very stable dependence of the velocity on $\sqrt{\sin(\theta)}$ implying a friction force that is proportional to the square of the velocity. The *faster* the disk moves, the *shorter* the time interval during which energy is fed into the system. If, on the other hand, one assumes, as in ballistic flight, that $\delta\tau$ is determined only by the perpendicular velocity, v_y, then one gets very unstable motion. The *faster* the disk, the *longer* the time interval during which energy is fed into the system and the more difficult it is to dissipate it. This drives the instability. In our simple model, the time of flight is given by both v_x and v_y depending on the side of the line beads that is impacted.

For small inclination angles, our model gives $\delta\tau$ that is dominated [20] by v_x as shown in Fig. 8(a) for $\sin(\theta)=0.03$. This gives a dependence on $\sin(\theta)$ that is very close to a square root, as is seen for the same angle in Figs. 3(a) and 3(b). The reason for this is that at such small angles, v_y is so small that the motion is mostly parallel to the line, i.e., in the x direction, which, as mentioned above, gives a $\sqrt{\sin(\theta)}$ dependence. For large values of θ, the motion is very bumpy, v_y is quite large, and it dominates the contribution to $\delta\tau$, as is seen in Fig. 8(c) for $\sin(\theta)=0.4$. At this value, we see that $\langle v_x \rangle$ increases faster than linearly with $\sin(\theta)$, Figs. 3(a) and 3(b), as the system is headed for the jumping regime C. In between the two regions of sublinear and superlinear dependence on $\sin(\theta)$, there is a region of competition between the v_x and v_y contributions to $\delta\tau$ as is seen in Fig. 8(b) for $\sin(\theta)=0.2$, which is in the heart of the linear regime. It is this competition between the destabilizing influence of v_y and the strong stabilizing influence of v_x that

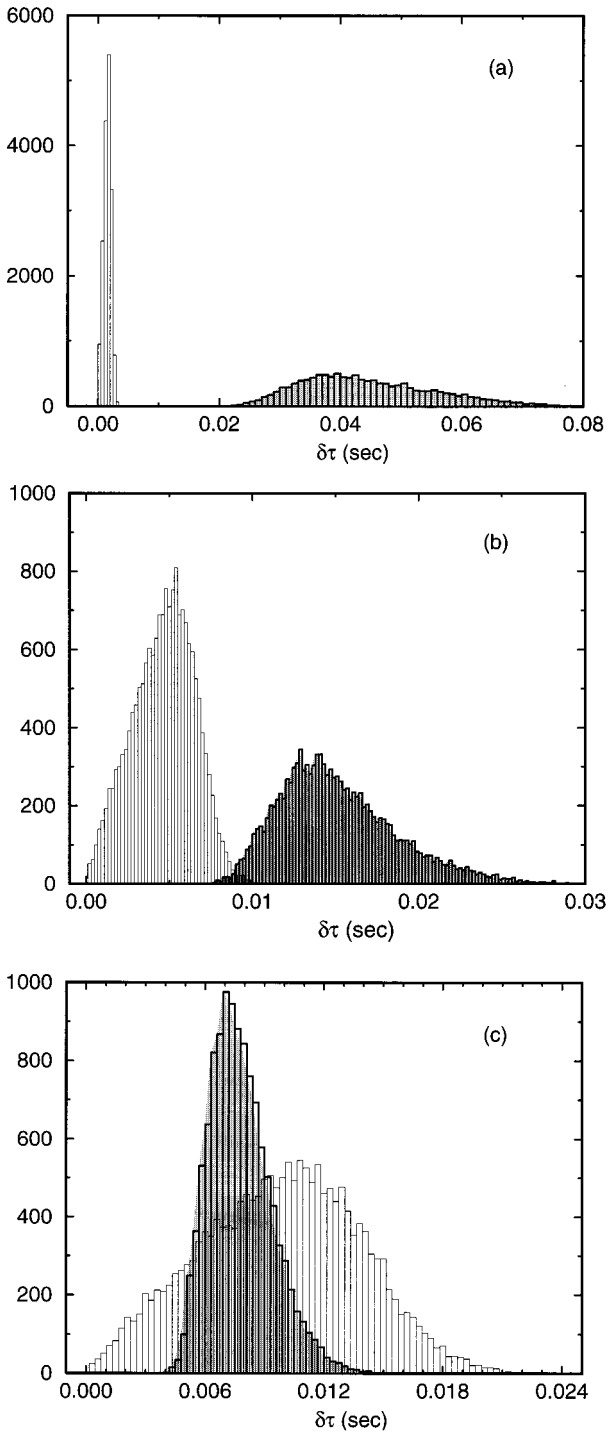

FIG. 8. (a) Histogram of times between bounces. The shaded histogram shows $\delta\tau$ for collisions at positive γ, i.e., where the time of flight is determined by v_x. The other histogram shows the case for negative γ, i.e., $\delta\tau$ is determined by v_y. $\sin(\theta)=0.03$, the other parameters are as in Figs. 3(a) and 3(b). (b) As in (a) but with $\sin(\theta)=0.2$. (c) As in (a) but with $\sin(\theta)=0.4$.

gives rise to the effective viscous friction and linear dependence on $\sin(\theta)$.

What about the scaling observed in Figs. 3(b) and 7? We found that if we use a tangential coefficient of restitution, μ_t, that is constant instead of as in Eqs. (9a) and (9b), the scaling exponent for Fig. 3(a) is 0, i.e., all the curves always overlap completely in the linear regime. Furthermore, we found that with this assumption, it is the *smaller* disks that enter the jumping regime C first, in clear contradiction with the experiments and intuition. Therefore the experimentally based Eqs. (9a) and (9b) are crucial to obtaining the correct behavior. On the other hand, we found that taking μ_t to be constant does not change the behavior in Fig. 7 (i.e., when $R/r=\text{const}$) by much: the exponent is changed from 0.5 to 0.43 and the scaling is still clearly visible. This interesting result indicates that although, in our model, the exponents for Figs. 3(b) and 7 are very similar, the two scaling effects appear to have different origins.

It is worth emphasizing that geometry is playing a dominant role in this model. The distribution of the stochastic variable, γ, given by Eqs. (7a) and (7b), is dominated by the velocity dependent shadows cast by disks on their neighbors, constraining the cross section available for collisions. In addition, this distribution is clearly crucial in deciding which of Eqs. (8a) or (8b) determines the time of flight whose role is discussed above. Because of all this, we see that the allowed collisions and the velocities are strongly dependent on the geometry, which also means that, because of Eq. (9a), μ_t is also dependent on the geometry.

IV. CONCLUSIONS

We have presented in this paper a stochastic model for the motion of a disk down an inclined line of smaller disks, separated by random distances. The stochastic equations are based on the original deterministic equations of motion to which we have added some simplifying assumptions. Our two main assumptions are that we can neglect rotation (supported by MD [12]), and that the motion of the disk is a series of small bounces, with one bounce per line disk (supported by recent experimental results on the two-dimensional plane [21] and by MD simulations [12]). This simple model, where geometry plays a very important role, accurately reproduces the features of the experimental data, and explains the origin of the viscous friction force. This is seen to be the result of competition between ballistic motion (with large v_y determining the time of flight) and motion parallel to the plane (where v_x determines the time of flight). We also emphasized the importance of the dependence of the tangential coefficient of restitution on the angle of incidence.

The next phase is to compare the results from this model with experiments currently being done on the stopping distance of the balls in regions A and B. The properties of the stopping distance in region B have very important industrial applications in the segregation of grains with different sizes. We will also compare with experiments the results of our model for the longitudinal dispersion of the velocity and its dependence on the sizes of the balls and the inclination angle. For the longer term, we would like to generalize the model to a two-dimensional plane, where we can make more quantitative comparisons with experiments including results for the transverse motion which is absent on a one-dimensional line.

ACKNOWLEDGMENTS

We wish to thank D. Bideau, Ph. de Forcrand, A. Hansen, C. Henrique, I. Ippolito, J. Schäfer, K. Taylor, and D. Wolf for very valuable discussions. G.G.B. and L.S. acknowledge support from the GdR CNRS ''Physique des Milieux Hétérogènes Complexes.''

[1] A. Rosato, K. J. Strandburg, F. Prinz, and R. H. Swendsen, Phys. Rev. Lett. **58**, 1038 (1987).
[2] M. B. Donald and B. Roseman, Brit. Chem. Eng. **7**, 749 (1962).
[3] R. Jullien and P. Meakin, Europhys. Lett. **4**, 1385 (1987); C. Ghidaglia, E. Guazzelli, and L. Oger, J. Phys. D **24**, 2111 (1991).
[4] J. B. Knight, H. M. Jaeger, and S. R. Nagel, Phys. Rev. Lett. **70**, 3728 (1993).
[5] R. Jullien and P. Meakin, Nature **344**, 425 (1990).
[6] F.-X. Riguidel, M. Ammi, D. Bideau, A. Hansen, and J.-C. Messager, in *Powders and Grains 93*, edited by C. Thornton (Balkema, Rotterdam, 1993).
[7] F.-X. Riguidel, A. Hansen, and D. Bideau, Europhys. Lett. **28**, 13 (1994).
[8] F.-X. Riguidel, Ph.D. thesis, University of Rennes 1 (1994).
[9] F.-X. Riguidel, R. Jullien, G. Ristow, A. Hansen, and D. Bideau, J. Phys. I (France) **4**, 261 (1994).
[10] In Refs. [6–8] the scaling is expressed as $(R/r)^{\alpha}$, but since the radius r of the beads on the plane is kept fixed, we will not use the ratio of the radii. Another reason for not doing that is that even with R/r fixed, changing R will change $\langle v \rangle$, as we will see later.
[11] See, for example, P. Le Doussal and V. M. Vinokur (unpublished).
[12] S. Dippel, G. G. Batrouni, and D. E. Wolf (unpublished).
[13] S. Dippel, L. Samson, and G. G. Batrouni, in *Proceedings of ''Traffic and Granular Flow'' Workshop*, edited by D. Wolf (World Scientific, Singapore, 1995).
[14] We can include the effects of the fluctuations in y, but the model becomes more cumbersome and the results do not change.
[15] S. F. Foerster, M. Y. Louge, H. Chang, and K. Allia, Phys. Fluids **6**, 1108 (1994).
[16] A. Aguirre, I. Ippolito, A. Calvo, C. Henrique, and D. Bideau, (unpublished).
[17] Clearly this can hold only within a certain range of parameters.
[18] G. Ristow, F.-X. Riguidel, and D. Bideau, J. Phys. I (France) **4**, 1161 (1994).
[19] C.D. Jan, H.W. Shen, C.H. Ling, and C.L. Chen, in *Proceedings of the 9th Conference on Engineering Mechanics, College Station, Texas*, edited by L. D. Lutes and J. M. Niedzwecki (American Society of Civil Engineers, New York, 1992), p. 768.
[20] By ''dominate'' we mean that most of the energy fed into the system is done during bounces whose duration is determined by one of the velocities, v_x or v_y.
[21] C. Henrique (private communication).